Cement & Concrete Composites 34 (2012) 1130–1140

Contents lists available at SciVerse ScienceDirect

Cement & Concrete Composites

journal homepage: www.elsevier.com/locate/cemconcomp

Influence of mesostasis in volcanic rocks on the alkali-aggregate reaction

Francieli Tiecher [a,*], Denise Carpena Coitinho Dal Molin [a], Márcia Elisa Boscato Gomes [b], Nicole Pagan Hasparyk [c], Paulo José Meleragno Monteiro [d]

[a] Department of Civil and Engineering, Universidade Federal do Rio Grande do Sul, Avenida Osvaldo Aranha, 99, Norie, no. 3, Centro, Porto Alegre/RS, CEP 90035190, Brazil
[b] Department of Geology, Universidade Federal do Rio Grande do Sul, Avenida Bento Gonçalves, 9500 Porto Alegre/RS, Brazil
[c] Department of Concrete and Quality Control, Furnas Centrais Elétricas, Avenida de Furnas, s/n, Aparecida de Goiânia/GO, Brazil
[d] Department of Civil and Environmental Engineering, University of California, Berkeley, CA 94720, USA

ARTICLE INFO

Article history:
Received 22 November 2011
Received in revised form 29 July 2012
Accepted 30 July 2012
Available online 16 August 2012

Keywords:
Volcanic rock
Mesostasis
Crystallinity
Reactivity
Quartz
Basalt
Rhyolite

ABSTRACT

Mesostasis material present in the interstices of volcanic rocks is the main cause of the alkali-aggregate reaction (AAR) in concretes made with these rock aggregates. Mesostasis often is referred to as volcanic glass, because it has amorphous features when analyzed by optical microscopy. However, this study demonstrates that mesostasis in the interstitials of volcanic rocks most often consists of micro to cryptocrystalline mineral phases of quartz, feldspars, and clays. Mesostasis has been identified as having different characteristics, and, thus, this new characterization calls for a re-evaluation of their influence on the reactivity of the volcanic rocks. The main purpose of this study is to correlate the characteristics of mesostasis with the AAR in mortar bars containing basalts and rhyolites.

© 2012 Elsevier Ltd. All rights reserved.

1. Introduction

The alkali-aggregate reaction (AAR) is a chemical reaction between silica from the concrete aggregates (rocks and sands) and alkaline hydroxides that form during the hydration process of Portland cement concrete. The by-product of this hydration is a hygroscopic gel. Water in the concrete promotes gel expansion and hence internal stresses, leading to cracks and deformation.

Even aggregates from basic rocks (those with a low silica content such as basalts), have proved highly reactive in accelerated tests to available aggregate reactivity. Their reactivity is usually ascribed to amorphous material (volcanic glass) present on the grains in the interstices [1–5]. Amorphous, or microcrystalline silica phases, generally react quickly with alkaline hydroxides because they dissolve readily [1,3,5–7]. According to Wakizaka [3], the following factors control silica dissolution in concrete aggregates: silica content, thermodynamic properties, specific surface, and crystallinity.

However, the material known as volcanic glass in most cases is not amorphous. Using scanning electron microscopy (SEM) in conjunction with energy-dispersive spectroscopy analysis (EDS), Gomes [8] showed the presence of small K–feldspar and quartz crystals in this interstitial material. According to the author, the chemical composition of mesostasis can vary widely. In these experiments [8], mesostasis of rocks had 47–80% silica (SiO_2) content, the K_2O was about 10%, Na_2O was 3%, and Al_2O_3 was 18%. Gomes [8] also found smaller amounts of MgO, CaO, and FeO.

Mesostasis is a residue from the sudden cooling of volcanic magma, which is alkali-silica rich and may have different composition of microcrystalline phases. The influence of the characteristics of mesostasis on the AAR has yet to be fully addressed. Although Tiecher [9] evaluated the amount of mesostasis in 14 basalts from southern region in Brazil, the expansion potential of these basalts was not determined. Moreover, there are few studies about the reactivity of volcanic rocks compared with metamorphic and plutonic rocks. Noteworthy are studies by Korkanç and Tuğrul [1], and Wakizaka [3].

The most frequent lithotypes of volcanic rocks are basalts and rhyolites. Basalts are usually classified as reactive rocks in accelerated mortar tests, but in concrete tests basalts are often assumed to be innocuous [10,11]. Rhyolites, in turn, have proved to be reactive in both tests and also in the field [12–16].

Mineral phases into mesostasis, as well as its degree of crystallinity may influence the AAR development in basalts and rhyolites. This study aims to evaluate the characteristics of mesostasis of different volcanic rocks and correlate them with reactivity of the rocks.

* Corresponding author. Tel.: +55 51 3308 3518; fax: +55 51 3308 4054.
E-mail address: francieli-tiecher@cientec.rs.gov.br (F. Tiecher).

0958-9465/$ - see front matter © 2012 Elsevier Ltd. All rights reserved.
http://dx.doi.org/10.1016/j.cemconcomp.2012.07.009

2. Experimental program

2.1. Methods

Mineralogical composition and texture of rocks were performed through petrographic analysis at transmitted light optical microscopy, scanning electron microscopy (SEM), and energy-dispersive spectroscopy analysis (EDS). Mineral phases and interstitial material (mesostasis) were measure by modal quantification on slides with 30 μm.

X-ray diffractometry was used for mineralogical characterization and identification of the crystalline phases. The powder method was used, passing sample fractions in #200. Clay minerals were identified through the suspension method in the oriented condition, according to the technique proposed by Alves [17]. This consists of separating clays from the rocks and then analyzing them through natural, calcined (500° for 2 h) and glycoled. A Siemens Bruker-AXS, model D5000 diffractometer with a θ–θ goniometer, Cu Kα (λ = 1.5418 Å) radiation, and graphite monochromator was used. Operating conditions of the X-ray tube were 40 kV and 25 mA. Acquisition time was 1 s per point with 0.02° pitch, with the sweep 2–72° (2θ scale) in the samples analyzed using the powder method and 2–28° (2θ scale) for the oriented samples. Chemical composition of rocks was determined by X-ray fluorescence spectrometry (XRF). Detailed analyses of the characteristics of mesostasis and its chemical/mineralogical composition were carried out with SEM and EDS. Backscattered images were obtained with a Jeol–JSM 5800 scanning electron microscope with an acceleration current of 20.0 kV. Thin carbon metalized slides were used for the analyses.

An accelerated mortar bar test—according to Brazilian standard NBR 15577-4 [18]—was used to characterize the alkali-reactivity of rock samples; this test is similar to ASTM C 1260 [19] and CSA A23.2-25A [20]. The three mortar bars were composed of 440 g of cement and 990 g of specific grain size aggregates that were mixed together. After molding, test bars (285 × 25 mm) were deposited in a wet chamber for 24 h and then placed in water at 80 °C for another 24 h. According to ASTM C 1260 [18], the mortar bars should have been immersed in 1 M NaOH solution at 80 °C for 28 days; however, the test was prolonged for an additional 100 days in order to observe behavior of rocks over the passage of time. Periodical measurement of the length of the bars was made during their immersion in alkaline solution. Mortar bars expansions above 0.19% at 28 days classified the aggregates as potentially reactive. ASTM C 1260 [18] specifies that 0.20% is the limit of expansion at 28 days of immersion.

Silica dissolution from rock samples was measured through the visible spectrophotometric method according to Brazilian Standard NBR 9848 [21] (the spectrophotometric method is similar to the method of the ISO 9874:1974 (E) [22]), which specifies the test method for silica determination in liquid caustic soda. This test is for determining the resulting color of the silica–molibdic (ammonia molibdate) complex at pH close to 1, which is formed through visible spectrophotometry. Silica concentration is proportional to the silica present. In order to perform the test, rock samples between 0.15 mm and 0.30 mm were submerged in a 1 M NaOH solution at 80 °C for 3 days. Afterward, the rocks were removed from the alkaline solutions and analyzed using the spectrophotometric method.

2.2. Materials

2.2.1. Rocks

The experiments reported herein used two different types of volcanic rocks—basalt and rhyolite—which have different mineralogical compositions. The basalt sample is a porphyritic rock composed of plagioclase, pyroxene, and phenocrystals of Fe–Ti oxide in a fine matrix of plagioclase (43.37%), pyroxene (35.22%), opaque minerals (4.58%), and mesostasis (16.83%), with traces of apatite and hematite (see Fig. 1a). The rhyolite sample is composed of K–feldspar (19.92%), quartz (23.72%), plagioclase (18.22%), pyroxene (7.72%), Ti–magnetite (3.18%), mesostasis (30.42%), traces of clay minerals, apatite, and hematite (see Fig. 1b).

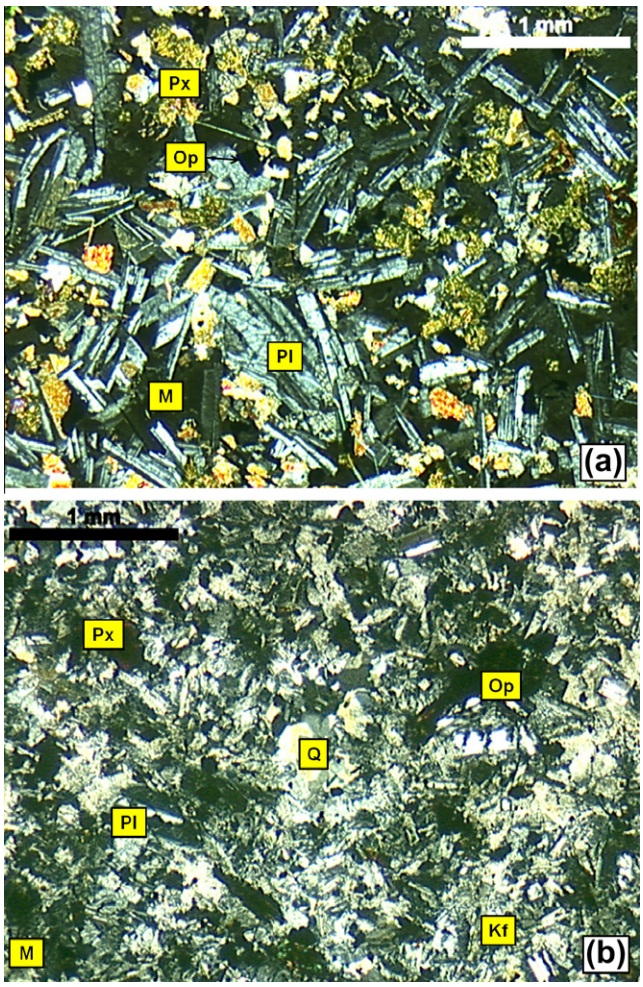

Fig. 1. Micrographs of (a) basalt and (b) rhyolite, obtained under optical microscopy with cross polarization, magnification = 25×, in which Pl = plagioclase, Px = pyroxene, Op = opaque minerals, Q = quartz, K–f = K–feldspar.

The XRD patterns (Figs. 2 and 3) of rock samples do not show signs of amorphous constituents. Note the presence of quartz in the XRD pattern of the basalt rock (Fig. 2a), which appears as submicroscopic grains, i.e., invisible to optical microscopy. Quartz in basalt occurs in mesostasis.

Figs. 2b and 3b present XRD patterns of the <2 μm fraction in the oriented condition identifying the clay minerals. A peak can be observed at about 15.0 Å, displaced towards to left (16.5 Å); after being saturated with ethylene–glycol it appears at 10.0 Å after calcination. This behavior is characteristic of expansive clay minerals of the smectite group. Previous studies of these rocks have concluded that clays are saponites [8,23], which are expansive in nature, possibly contributing to concrete expansion.

Chemical analyses of the rocks (see Table 1) demonstrated that the basalt sample had around 54% SiO_2, which is compatible with a

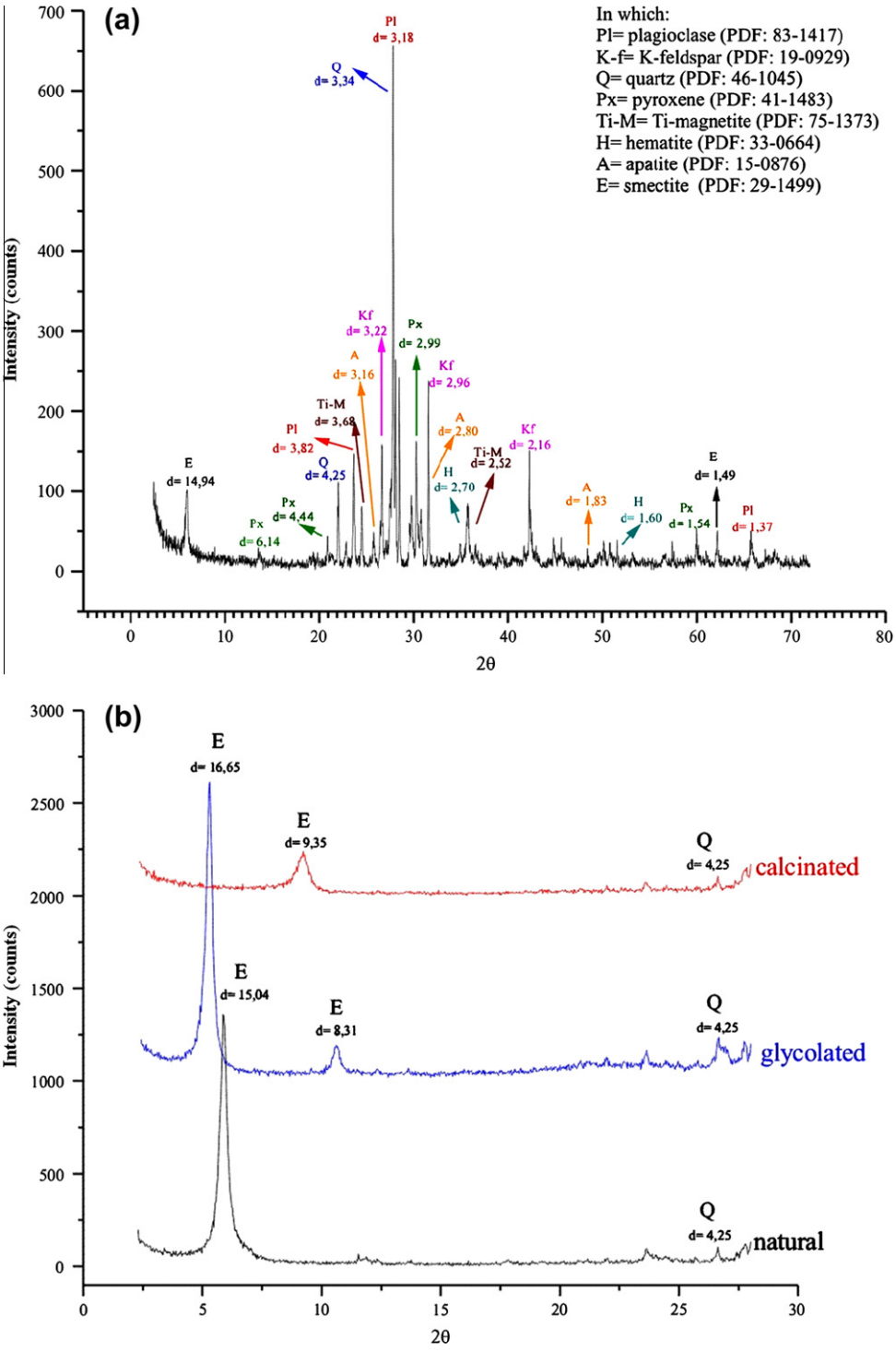

Fig. 2. XRD patterns of the basaltic rock (a) and clay minerals (b).

toleitic nature. An excess of SiO_2 in basalt rock forms microcrystalline quartz into residue with the fast crystallization of magma (mesostasis). Rhyolite, however, is composed of 68% SiO_2, which composes quartz crystals in the rock matrix and microcrystalline quartz into mesostasis.

Various researchers [24–26] have proposed that the Na_2O and K_2O present in rock samples could contribute to the AAR. Sodium in rock samples constitutes the plagioclase and excess crystallized microcrystalline phases in mesostasis, a similar reaction occurs with potassium (K) from the K–feldspar in the rhyolite sample. There are no main potassium minerals in the basalt rock, however, and the potassium found in basalt is from microcrystalline K–feldspars in mesostasis. All the microcrystalline phases in mesostasis are highly soluble in alkaline environments to their "unstable" condition, thus, they contribute to increase the alkalinity of the concrete pores, causing greater predisposition to the AAR.

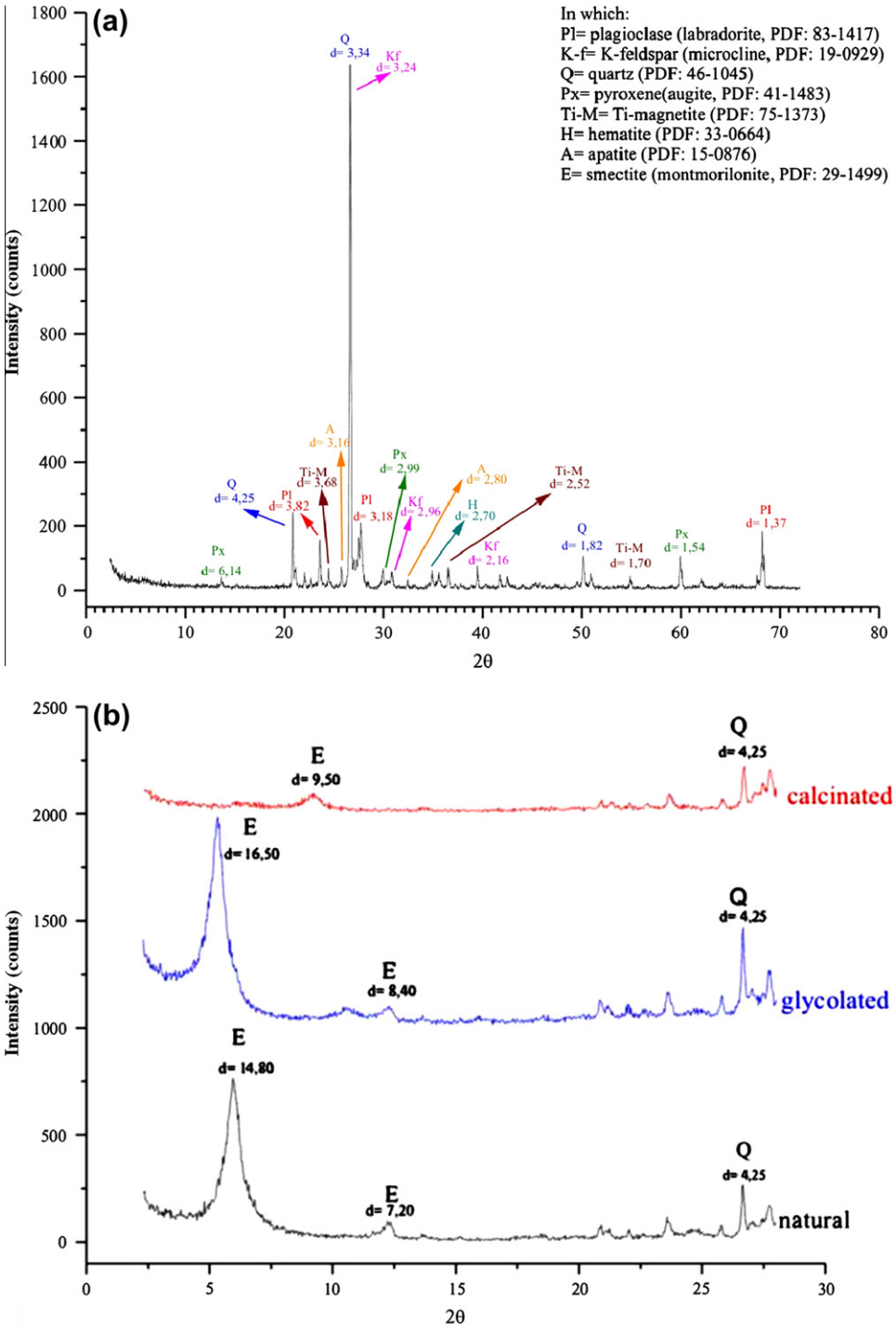

Fig. 3. XRD patterns of the rhyolitic rock (a) and clay minerals (b).

2.2.2. Cement characterization

Accelerated mortar bar tests were performed on a sample made with pure Portland cement and classified as CPI according to Brazilian standard NBR 5732 [27] (which is similar to Type I according to American standard ASTM C 150 [28]). The cement used conformed to the standards for accelerated mortar bar tests: the samples had a total alkali content $Na_2Oeq = 0.89\%$; specific area = 4920 cm^2/g; autoclave expansion = 0.02%, and no additions of any kind.

3. Results

3.1. Characterization of mesostasis

As previously mentioned mesostasis is a residual material, composed of microcrystalline minerals from fast-cooling magma and are found in volcanic rocks. Under optical microscopy, mesostasis has features of amorphous material; consequently, it is called volcanic glass.

Table 1
Chemical composition of the rocks (% mass).

Compound	Basalt	Rhyolite
SiO_2	54.04	67.98
Al_2O_3	16.71	11.75
TiO_2	0.94	1.15
Fe_2O_3 (total)	10.33	7.32
MnO	0.18	0.12
MgO	4.81	0.74
CaO	9.22	2.38
Na_2O	1.73	1.89
K_2O	1.39	4.15
P_2O_5	0.14	0.18
Loss to fire	0.70	1.015
Total	100.21	98.68

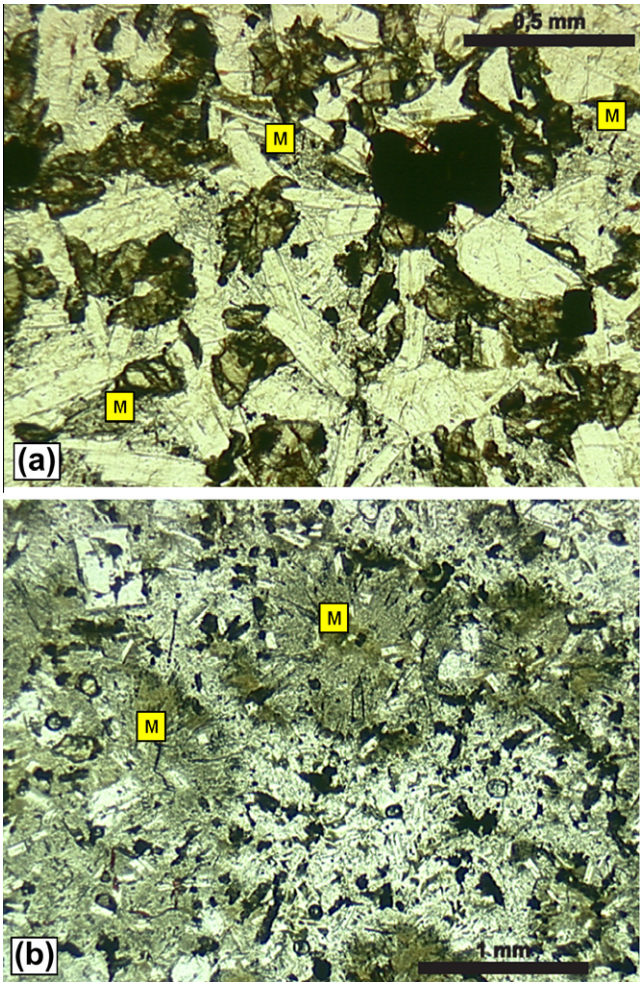

Fig. 4. Micrographs of (a) basalt and (b) rhyolite, obtained in optical microscopy under natural light, magnification = 25×, in which M = mesostasis.

Fig. 4 compares the textures of the rock samples, showing the distribution of mesostasis in both of them. Note that the rhyolite sample shows sites with large volume of this interstitial material, which is characterized by radiating texture and dark color and is not present in the basalt sample. As shown in Table 2, petrographic analysis showed three different categories of mesostasis, which are present in basalt and rhyolite: (a) containing microcrystalline grain (Mn); (b) with better crystallized grains (Mq); and (c) with predominantly clay minerals (Ma).

Table 2
Characteristics of mesostasis.

Type of mesostasis	Characteristic description	Micrographies (transmitted light optical microscope)	
		Natural light	Cross polarizer
Mesostasis consisting of microcrystalline grains (Mm)	Low crystallinity material, rich in silica and alkalis, accompanied by small grains of hematite and apatite needles. No quartz or feldspar grains can be observed by optical microscopy	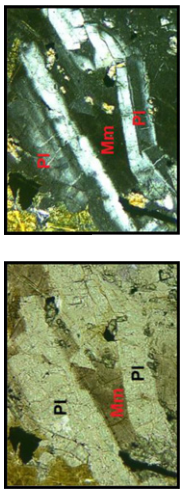	
Mesostasis with better crystallized grains (Mq)	Dissemination of quartz grains, which can be seen in optical microscopy, associated with feldspar and small quantities of clay minerals and apatites	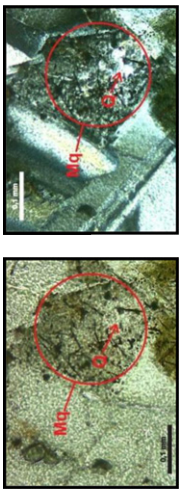	
Mesostasis with predominant clay minerals (Ma)	Greenish mesostasis in which clay minerals (smectite) are predominant. Small quantity of quartz-feldspar material	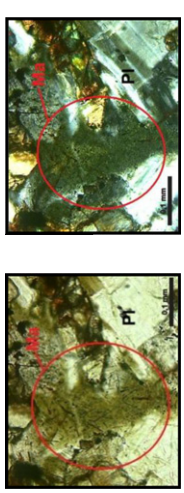	

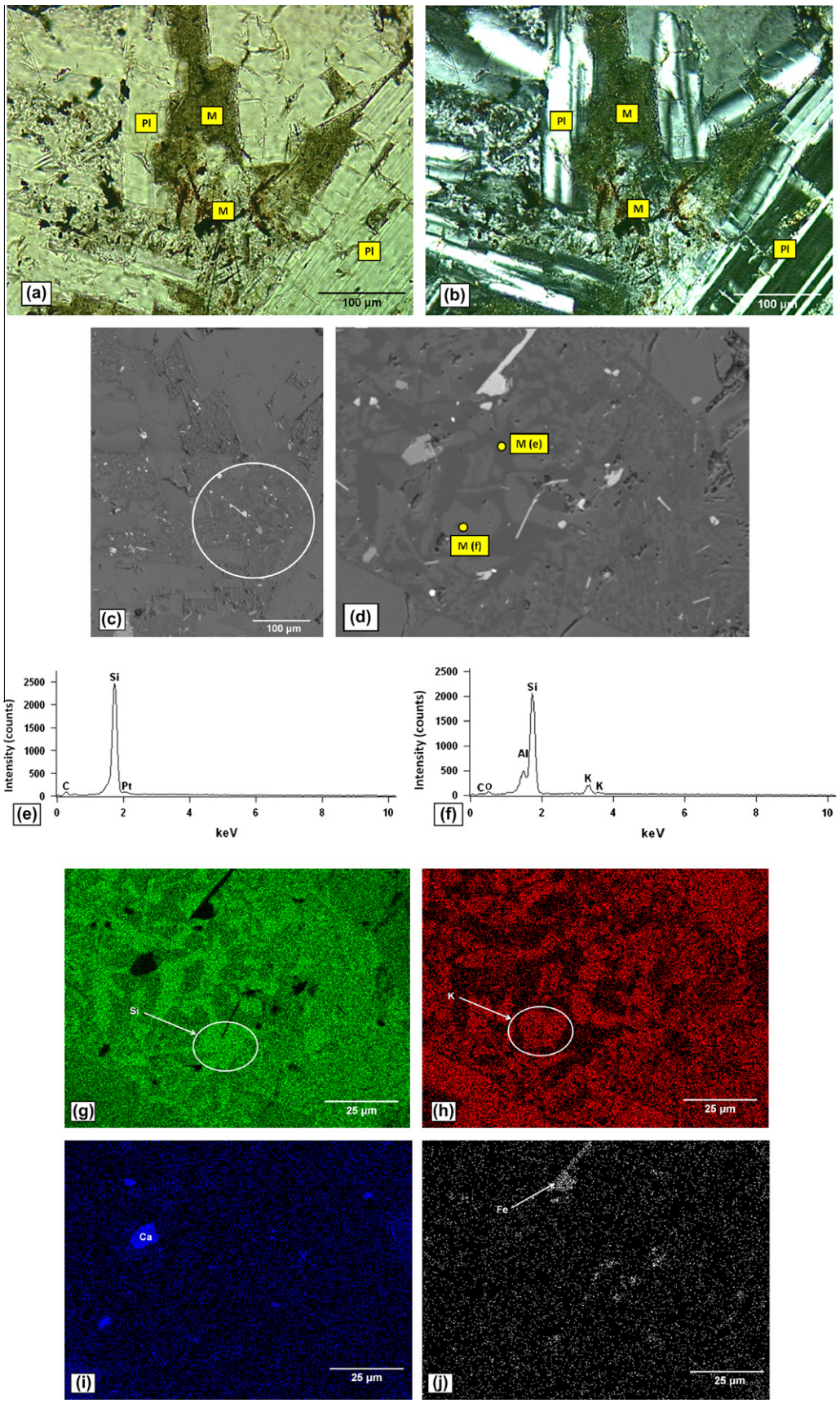

Fig. 5. Micrographs of Mm mesostasis, obtained by optical microscopy under natural light (a), cross polarization (b) (magnification = 100×) and SEM through backscatter electron beam (c) (d) (magnification = 300×; 1000×); EDS spectrum of the quartz (e) and K–feldspar of Mm mesostasis (f); map of Si (g), K (h), Ca (i); Fe (j), in which Mm = mesostasis with microcrystalline grain, Px = pyroxene, Si = region where silica (quartz) is found, Fe = region where Fe (pyroxene) is found, Ca = region where calcium (pyroxene and plagioclase) is found, K = region where potassium (K–feldspar) is found.

Table 3
Free silica component of the rocks, before and after the accelerated expansion test (%).

Type of mesostasis	Samples			
	Basalt		Rhyolite	
	Before test	After test	Before test	After test
Quartz	–	–	23.7	11.8
Mm mesostasis	7.7	2.0	16.1	3.8
Mq mesostasis	3.6	0.3	6.1	1.0
Ma mesostasis	5.5	5.3	5.0	5.0
Total	16.8	7.6	27.2	9.8

Different categories of mesostasis were observed by SEM and analyzed by EDS. It was found that Mm mesostasis transmitted low light at optical microscopy, where no crystals could be distinguished (Fig. 5a and b). The backscattered SEM image shows two tones of gray Fig. 5c); the darkest is quartz, as shown in Fig. 5d and e, the lightest is K–feldspar, as shown in Fig. 5d and f. If this was an amorphous material, the silica would not be decoupled from alkalis.

The map of elements in Mm mesostasis, (acquisition time equals 20 min, detection time equals 50 s, acceleration voltage

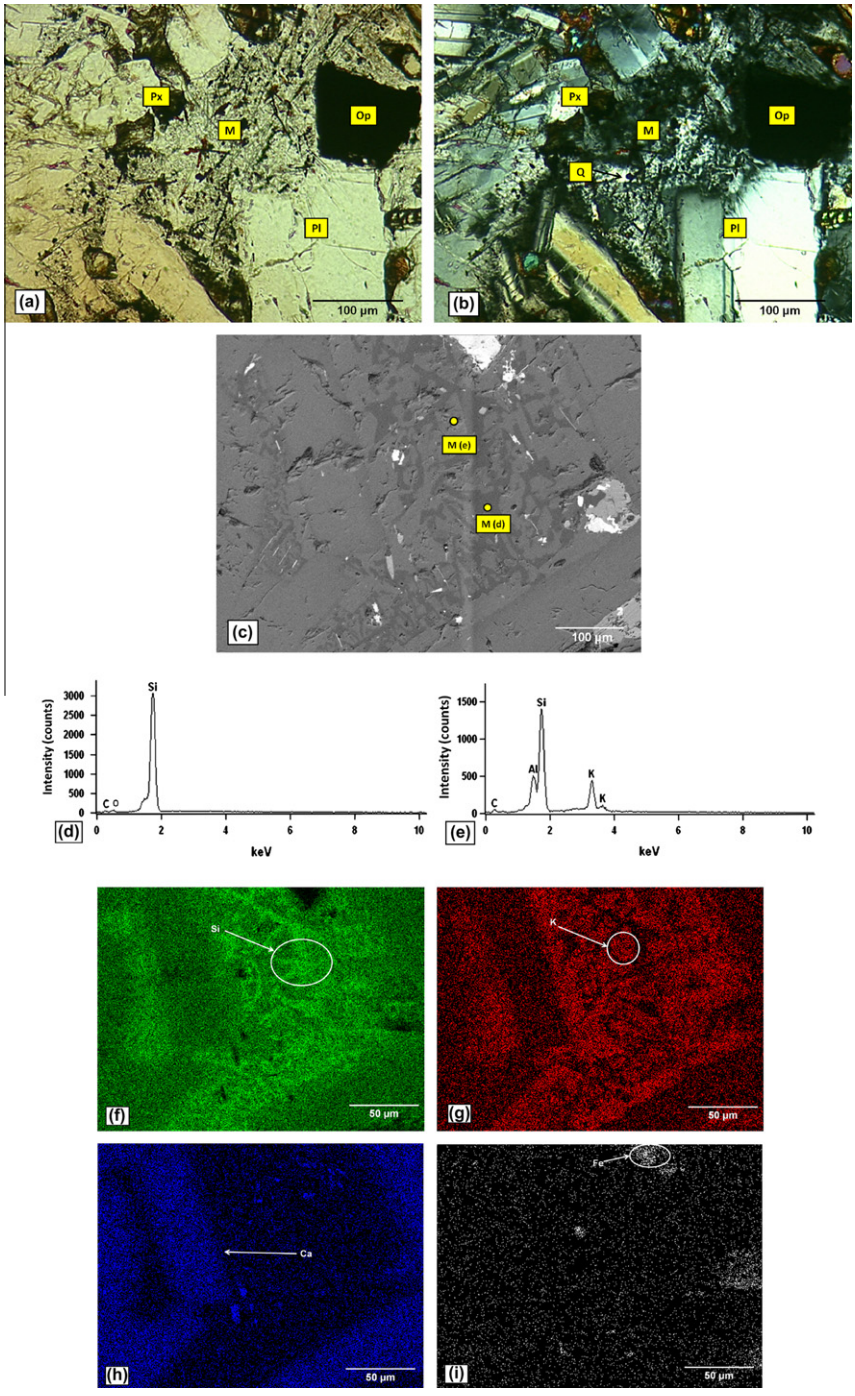

Fig. 6. Micrographs of Mq mesostasis, obtained by optical microscopy under natural light (a), cross polarization (b) (magnification = 100×) and SEM through backscatter electron beam (c) (magnification = 400×); EDS spectrum of the quartz (d) and K–feldspar of Mq mesostasis (e); map of Si (f), K (g), Ca (h); Fe (i), in which Mq = mesostasis with finer crystallized grains of quartz and feldspars, Px = pyroxene, Si = region where silica (quartz) is found, Fe = region where Fe (pyroxene) is found, Ca = region where calcium (pyroxene and plagioclase) is found, K = region where potassium (K–feldspar) is found.

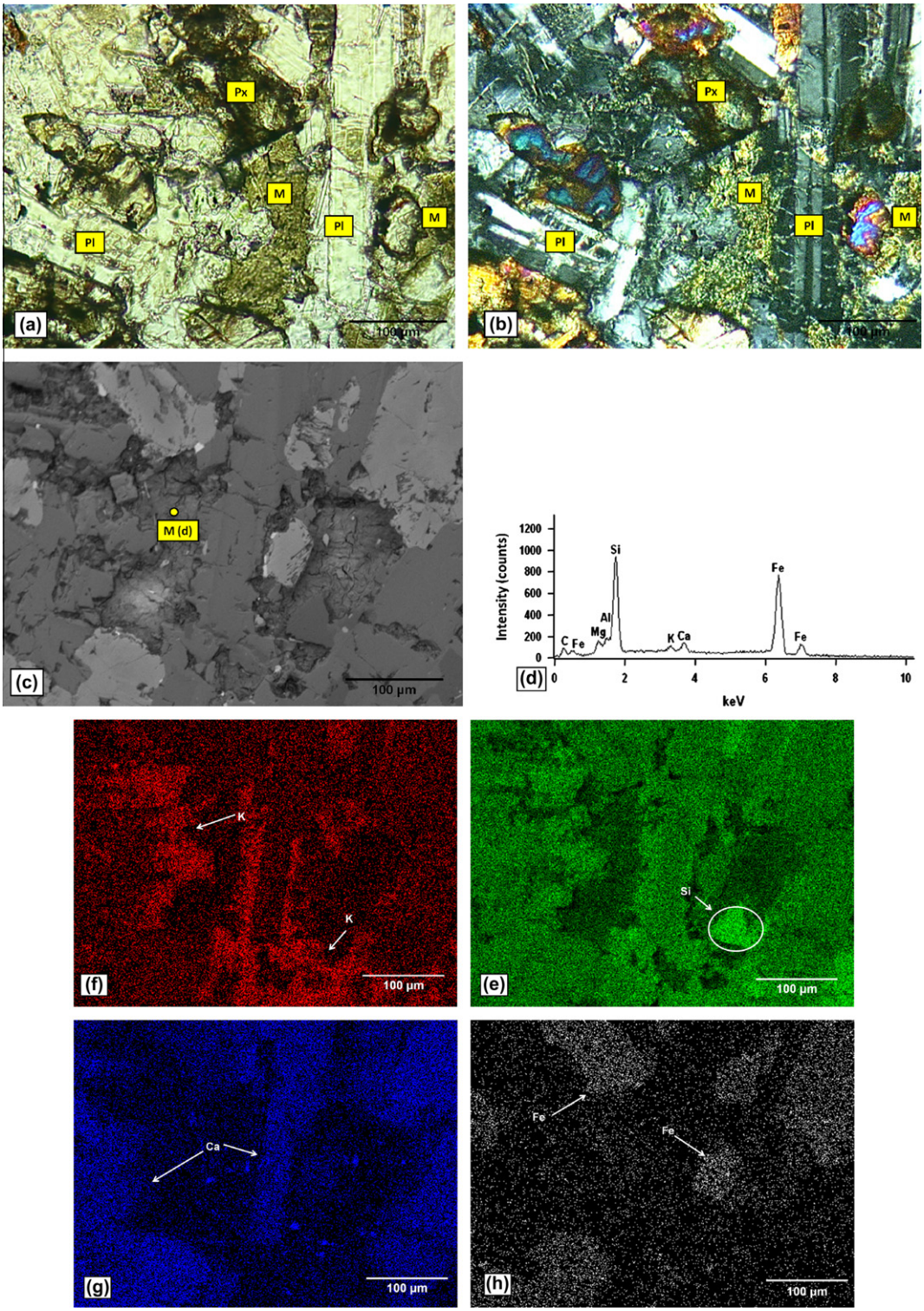

Fig. 7. Micrographs of Ma mesostasis, obtained by optical microscopy under natural light (a), cross polarization (b) (magnification = 200×) and SEM through backscatter electron beam (c) (magnification = 300×); EDS spectrum of the quartz (d) and K–feldspar of Mq mesostasis (e); map of Si (f), K (g), Ca (h); Fe (i), in which Ma = mesostasis with clay minerals, Px = pyroxene, Si = region where silica (quartz) is found, Fe = region where Fe (pyroxene) is found, Ca = region where calcium (pyroxene and plagioclase) is found, K = region where potassium (K–feldspar) is found.

equals 10 kV) showed regions with large Si concentration and the absence of additional elements (K, Ca and Fe), which indicate the presence of pure SiO_2 micrograins Fig. 5g), i.e., quartz. Other regions have K–feldspar (K mapping – Fig. 5h). In both rocks the quartz and K–feldspar grains present are smaller than 1 µm for both basalt and rhyolite' all regions with Mm mesostasis have these characteristic. Noteworthy to mention is the quartz and K–feldspar in basalt occur only in mesostasis and are not part of the main rock mineralogy.

Mm mesostasis contains irrelevant quantity of clay minerals (in both rocks), as can be deduced by the absence of Fe and Ca, since the clays identified in the rocks are saponites (see Section 2.2.1)

[8,23]. Fig. 5i and j illustrate the analysis made herein. Regions with Ca and Fe correspond to pyroxene, and those with Ca without Fe indicate the presence of plagioclase.

Mq mesostasis, which has better crystallized grains, was observed in both rocks, but was not as prominent in the basalt sample [see Table 3 (Section 3.2)]. This mesostasis is characterized by the presence of quartz and K–feldspar grains that can be seen at optical microscopy, as illustrated in Fig. 6a and b. In SEM with EDS assistance, it was also possible to identify grains constituting Mq mesostasis (Fig. 6c–e). The chemical map in Mq mesostasis (acquisition time equals 20 min., detection time equals 50 s, and acceleration voltage equals 10 kV) shows Si and K homogeneously distributed, with quartz and K–feldspar crystals identified by the higher concentration of Si and K, respectively (Fig. 6f and g).

Ma mesostasis is composed of predominantly clay minerals (more than 50% of the mesostasis) and is greenish under the natural light of an optical transmission microscope (Fig. 7a). Under cross polarization a dark slightly shiny material is observed (Fig. 7b). The SEM observations show that Ma mesostasis has a scaly appearance, which is very different from Mm and Mq mesostasis. This feature is due to lamellar habit of clay minerals and their very small size (Fig. 7c). Using EDS, the constituents of the clays were identified (Na, K, Ca, Al, Mg, and Si), which corroborates the petrographic analyses that showed main incidence of clay minerals instead of quartz and K–feldspars (Fig. 7d). The mapping of the chemical elements in Ma mesostasis confirmed that the K and Fe were predominant Fig. 7f and h); however, small pockets of highly concentrated Si are identified, showing that Ma mesostasis also presents microcrystalline quartz grains, although in less quantity (Fig. 7e).

3.2. Analysis of the potential development of the AAR

The accelerated mortar bar test was performed according to Brazilian standard NBR 15577-4 [18] (similar to US standard ASTM C 1260 [19]) to correlate the characteristics of mesostasis with expansion due to the AAR from volcanic rocks. Fig. 8 shows the expansion over time and that both the basalt and rhyolite samples are potentially reactive according to classification of the NBR 15577-1 [29] testing for Part 4, whereby aggregates are deemed potentially reactive when their expansions are above 0.19% at 30 days (ASTM C 33 [30] has a similar criterion).

Although both rocks are potentially reactive, Fig. 8 shows that basalt sample expanded 26% more than rhyolite at 30 days (basalt = 0.62%; rhyolite = 0.46%). Over time, however, the rate of the expansion of the basalt sample tended to stabilize. After 50 days, it was almost identical to the rhyolite expansion (basalt = 0.76%; rhyolite = 0.75%). At 100 days the rhyolite sample had expanded 65% more than basalt sample (basalt = 0.90%; rhyolite = 1.49%).

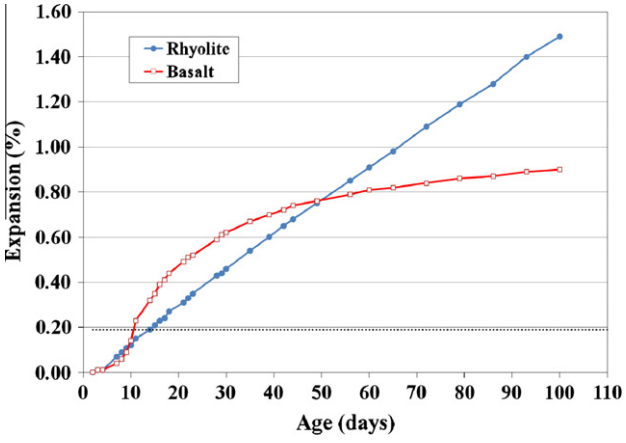

Fig. 8. Expansion over time – accelerated test of the mortar bar expansion.

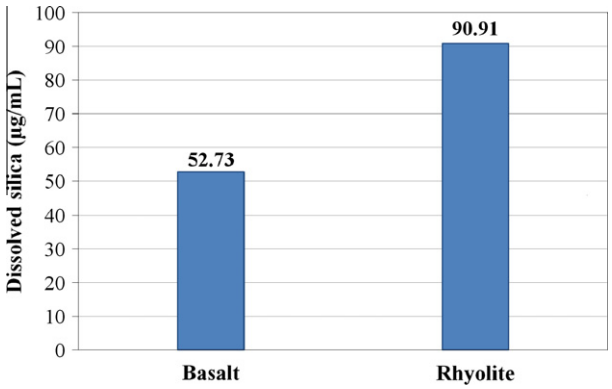

Fig. 9. Silica dissolution – visible spectrophotometric method (NBR 9848).

Considering the average expansion rates up to 30 days, the rate of expansion for the basalt sample was 0.21%, every 10 days, but from 30 to 100 days it fell to 0.04%. In contrast, the rhyolite sample's rate of expansion was linear; about 0.15%. Other researchers have also noted this phenomena for basalts when subjected to accelerated expansion tests [9,10,31].

According to results of the spectrophotometric test that evaluated silica dissolution of the rocks (Fig. 9), rhyolite enabled more silica dissolution than basalt, which explains its higher reactivity compared to basalt. At 30 days (the age prescribed by the standards [19,29]), however, the basalt could be considered more reactive.

Table 1 presents the chemical composition of the rocks, showing that rhyolite contained about 26% more silica than basalt. In rhyolite, silica is more available to react with other chemicals since its quartz comes from the matrix and from mesostasis. On the other hand, the silica found in basalt is from silicates such as plagioclase and pyroxene, which is combined with Ca, Al, Fe among others elements. Therefore, only a small portion of silica is "free" in basalts and corresponds to interstitial quartz into mesostasis, as observed at Section 3.1.

Quartz and K–feldspars are part of the main mineralogy of rhyolite rocks; therefore, mesostasis in rhyolite are under greater 'equilibrium' conditions unlike basalt. This 'equilibrium' is demonstrated by the lower expansion rate for rhyolite than basalt. The alkaline fluid in contact with rhyolites most likely reacts before with quartz (crypto-microcrystalline) from mesostasis and, as time passes, with quartz from the main matrix. Therefore, the rate of expansion during the accelerated test made with rhyolite remains identical from the beginning to the end of the test.

Fragments of rock samples immersed in mortars for the accelerated expansion test were analyzed through optical microscopy, SEM, and EDS. Modal analysis at optical microscopy allowed for quantifying the presence of quartz and mesostasis that remained after the accelerated test; note that the modal analysis was made during the same condition before and after the AAR (i.e., 2000 points per area). Table 3 lists the amounts of quartz and mesostasis from basalt and rhyolite before and after the accelerated expansion test.

As shown in Table 3, in the basalt sample 74% of Mm mesostasis and 91.7% of Mq mesostasis had dissolved, i.e., almost all quartz present in the basalt had dissolved, which explains the stabilization of expansion rate during the accelerated test (100 days). At the end of the test, 54.8% of the total mesostasis in the basalt had dissolved; most of remainder (45.2%) was Ma mesostasis, which is predominantly clay. Fig. 10 shows a basalt fragment after the accelerated expansion test, demonstrating

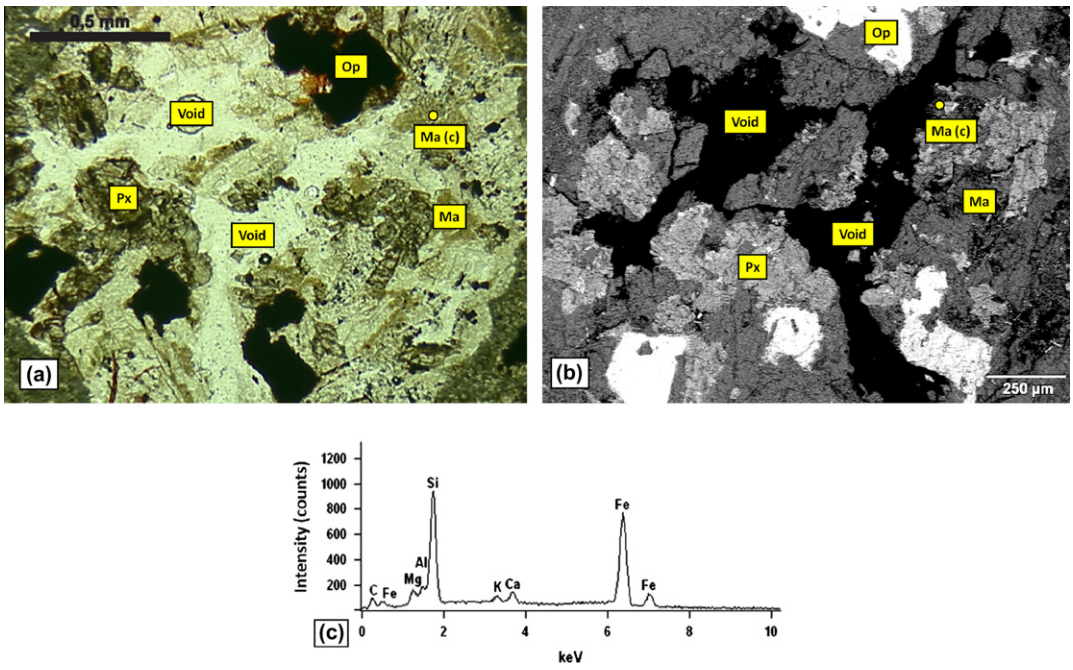

Fig. 10. Micrographs obtained through optical microscopy under natural light (a) (magnification = 50×) and through SEM by backscatter electron beam (b) (magnification = 80×); EDS spectrum of clay minerals of Ma mesostasis (c), in which Ma = mesostasis with the predominance of clay minerals, Op = opaque minerals, and Void = void in the interstitial of rock grain.

the predominance of the clay minerals from Ma mesostasis after the accelerated test.

According to analysis of the rock fragments after the accelerated mortar bar test, Ma mesostasis, which is found in smaller proportions in the original rocks matrix, is less sensitive to alkaline attack and dissolution. The aggressive conditions of the accelerated test enable dissolution of available silica in both rocks, but quartz from Ma mesostasis is protected by the clay minerals. In view of the easy availability of the quartz from other mesostasis, Ma mesostasis are less 'important' in the scale of dissolution, i.e., the clay acts as an "armor." Under the continuous aggressive conditions of the accelerated expansion test, it is assumed that the Ma mesostasis will dissolve.

Microcrystalline grains of quartz and K–feldspar in mesostasis are not part of the main mineralogy of the basalts. Being unstable, they are strongly susceptible to alteration by alkaline fluid in the concrete. Alkaline fluid reacts easily, rapidly, and powerfully with mesostasis in basalt, but because of amount of available silica is low (the amount of quartz in basalt is only found in mesostasis), the expansion due to the AAR soon stabilizes. Results obtained from the accelerated expansion test and silica dissolution support this conclusion, which is collaborated by the lack of reports from the field regarding basalts reactivity.

Table 3 shows that after exposure of the rocks to the alkaline solution (the accelerated expansion test) just 50.2% of quartz grains from rhyolite fragments (into mortars) had dissolved, but Mm and Mq mesostasis had dissolved 76.4% and 83.6%, respectively. Rhyolite had dissolved 64.0% of its total "free" silica, but around 50.0% of the quartz remained undissolved, and, consequently, the expansion rate of the mortar bars made with rhyolite did not stabilize, which was only exacerbated because rhyolite has much more silica available to "react" than the basalt sample.

4. Conclusions

Generally, the reactivity of volcanic rocks has been attributed to volcanic glass present in the interstices of the minerals. However, in this study it was concluded that material called volcanic glass is mostly composed of crypto-microcrystalline mineral phases: mesostasis.

Mesostasis has amorphous features when studied with optical microscopy, but through the use of SEM and EDS it is possible to identify mineral phases. Mesostasis may have several different characteristics that might influence the development of the AAR. Three mesostasis categories were determined in this study; the most important difference between them was the size of the grain, as they have same mineralogical composition; although with different amounts: Mm mesostasis has smaller grains than others mesostasis, and no quartz or feldspar was observed by optical microscopy; Mq mesostasis has larger grains of quartz and K–feldspar that are occasionally identifiable at optical microscopy; and Ma mesostasis is predominantly clay.

This study concluded that quartz grains from mesostasis are the main provider of silica dissolution when an alkaline volcanic rock, such as basalt, is close to an alkaline solution. Previous studies that have focused on the AAR in basaltic rocks have done so in laboratory conditions using accelerated expansion tests to document this reaction. These test results seem to contradict field reports in the literature where the AAR in concretes with basaltic aggregates does not occur. Consequently, it is possible to conclude that amount of quartz in basalts is not significant enough to promote the AAR in real situations. Accelerated expansion tests require very aggressive conditions (high alkalinity and temperature), which causes rapid dissolution of the microcrystalline quartz from mesostasis, as observed by the rapid intense initial expansion and immediate stabilization.

Acid volcanic rocks such as rhyolites have greater potential to be more damaging to real concrete structures because the amount of available silica to promote the AAR is larger. In rhyolites, the silica that dissolves is from both the quartz of the mesostasis and quartz of the matrix. Therefore it was concluded that amount of available silica (quartz) in volcanic rocks used in the production of concrete is critical in order to predict their reactivity.

Volcanic rocks are very complex. Often they have chemical composition and mineral compositions similar. Thus a greater

number of samples are being studied to get more results and in the future they will be published.

Acknowledgments

The authors of this study wish to thank the Centro de Microscopia Eletrônica (CME) of Universidade Federal do Rio Grande do Sul (UFRGS), the Conselho Nacional de Desenvolvimento Científico e Tecnológico (CNPq) and Furnas Centrais Elétricas S.A/ANEEL for their support to this research.

This publication was based on work supported in part by Award No. KUS-l1-004021, made by King Abdullah University of Science and Technology (KAUST).

References

[1] Korkanç M, Truğrul A. Evaluation of selected basalts form the point of alkali-silica reactivity. Cem Concr Res 2005;35:505–12.
[2] Goguel R. Alkali release by volcanic aggregate in concrete. Cem Concr Res 1995;25:841–52.
[3] Wakizaka Y. Alkali-silica reactivity of Japanese rocks. Eng Geol 2000;56:211–21.
[4] Valduga L, Dal Molin DCC, Paulon VA. Basalts potential reactivity survey in Brazil. In: Proceedings of the 2nd Simpósio sobre reação álcali-agregado em estruturas de concreto, Rio de Janeiro, Brazil; 2006.
[5] Tiecher F, Gomes MEB, Dal Molin DCC, Hasparyk NP, Monteiro PJM. Influence of microcrystalline material into volcanic rocks for alkali-aggregate reaction. In: Proceedings of the 59th Congresso Brasileiro do Concreto, Curitiba, Brazil; 2009.
[6] Broekmans MATM, Jansen JBH. Silica dissolution in impure sandstone: application to concrete. J Geochem Explor 1998;62:311–8.
[7] Leemann A, Holzer L. Alkali-aggregate reaction: identifying reactive silicates in complex aggregates by ESEM observation of dissolution features. Cem Concr Res 2005;27:796–801.
[8] Gomes MEB. Mécanismes de refroidissement, structurat et processus post-magmatiques des basaltes du bassin du Paraná – region de Frederico Westphalen (RS) – Brésil. Doctoral Thesis, Universidade Federal do Rio Grande do Sul; 1996.
[9] Tiecher F. Alkali-aggregate reaction: evaluation on the behavior of the aggregates from southern region of Brazil when different types of Portland cements are applied. Masters of Science Thesis, Universidade Federal do Rio Grande do Sul; 2006.
[10] Couto TA. Alkali-aggregate reaction: a study of the phenomenon in siliceous rocks. Masters of Science Thesis, Universidade Federal de Goiás; 2008.
[11] Sanchez LM. Contribution to the study of test methods in assessing alkali-aggregate reactions in concrete. Master of Science Thesis, Universidade de São Paulo; 2008.
[12] Duncan MAG, Gillot JE, Swenson EG. Alkali-aggregate reaction in Nova Scotia: field and petrographic studies. Cem Concr Res 1973;3:119–28.
[13] Berra M, Mangiardi T, Polini AE. Rapid evaluation of the threshold alkali level for alkali-reactive siliceous aggregates in concrete. Cem Conc Comp 1999;21:325–33.
[14] Katayama T, Tagamia M, Saraia Y, Izumib S, Hirab T. Alkali-aggregate reaction under the influence of deicing salts in the Hokuriku district. Jpn Mater Charact 2004;53:105–22.
[15] Shirimer FH. Progress in the evaluation of alkali-aggregate reaction in concrete construction in the Pacific Northwest, United States and Canada. In: Contributions to industrial-minerals research, Reston, USA; 2005.
[16] Marfil SA, Maiza P. Deteriorated pavements due to the alkali-silica reaction: a petrography study of three cases in Argentina. Cem Concr Res 2001;31:1017–21.
[17] Alves DB. Desenvolvimento da metodologia de preparação de amostras para análise difratométrica de argilominerais no centro de pesquisas da Petrobrás. Boletim de Geociências da Petrobrás 1987;1(2):157–75.
[18] Associação Brasileira de Normas Técnicas. NBR 15577-4: Agregados – Reatividade álcali-agregado – Parte 4: Determinação da expansão em barras de argamassa pelo método acelerado; 2008.
[19] American society for testing and materials. ASTM C 1260-01: Standard test method for potential alkali reactivity of aggregates (mortar-bar method); 2001.
[20] Canadian standards association. CSA A23.2-25A: test method for detection of alkali-silica reactive aggregate by accelerated expansion of mortar bars; 2009.
[21] Associação Brasileira de Normas Técnicas. NBR 9848: Soda cáustica líquida – Determinação de sílica – método espectrofotométrico visível com molibdato de amônio; 2004.
[22] International organization for standardization. ISO 9874-1974 (E): Sodium hydroxide for industrial use – determination of silica content – reduced silico-molibydic photometric method; 1974.
[23] Frank HT, Gomes MEB, Formoso MLL. Review to the areal extent and the volume of the Serra Geral Formation – Paraná Basin, South America. Pesquisas em Geociências 2009;36:49–57.
[24] Gillott JE, Rogers CA. Alkali-aggregate reaction and internal release of alkalis. Mag Conc Res 1994;46:99–112.
[25] Constantiner D, Diamond S. Alkali release from feldspars into pore solutions. Cem Concr Res 2003;33:549–54.
[26] Wang Y, Yu G, Deng M, Tang M, Lu D. The use of thermodynamic analysis in assessing alkali contribution by alkaline minerals in concrete. Cem Concr Compos 2008;30:353–9.
[27] Associação Brasileira de Normas Técnicas. NBR 5732: Cimento Portland comun – especificação; 1991.
[28] American society for testing and materials. ASTM C 150-97a: Standard specification for Portland cement. Annual Book of ASTM Standards; 1997.
[29] Associação Brasileira de Normas Técnicas. NBR 15577-1: Agregados – Reatividade álcali-agregado - Parte 1: Guia para avaliação da reatividade potencial e medidas preventivas para uso de agregados em concreto; 2008.
[30] American society for testing and materials. ASTM C 33-08: Standard specification for concrete Aggregates; 2008.
[31] Valduga L. Influence of ASTM C 1260 test conditions to verify alkali-aggregate reaction. Doctoral Thesis, Universidade Federal do Rio Grande do Sul; 2007.